

Thermodynamics of the spin-flop transition in a quantum XYZ chain

X. Wang and X. Zotos

Institut Romand de Recherche Numérique en Physique des Matériaux (IRRMA), PPH-Ecublens, CH-1015 Lausanne, Switzerland

J. Karadamoglou and N. Papanicolaou

Department of Physics, University of Crete, and Research Center of Crete, Heraklion, Greece

A special limit of an antiferromagnetic XYZ chain was recently shown to exhibit interesting bulk as well as surface spin-flop transitions at $T = 0$. Here we provide a complete calculation of the thermodynamics of the bulk transition using a transfer-matrix-renormalization-group (TMRG) method that addresses directly the thermodynamic limit of quantum spin chains. We also shed some light on certain spinwave anomalies at low temperature predicted earlier by Johnson and Bonner.

75.10.Jm, 75.30.Kz

There has been a revival of interest in bulk and surface spin-flop transitions following some recent experimental work on Fe/Cr multilayers.¹ These are effectively described by classical spin chains characterized by antiferromagnetic exchange interaction in addition to single ion anisotropy. It is then natural to raise similar questions in the context of quantum spin chains which are more appropriate for the study of quasi-one-dimensional crystalline magnetic systems.

Indeed, in a recent communication,² this issue was studied within a special limit of the spin- $\frac{1}{2}$ XYZ chain defined by the Hamiltonian

$$W = - \sum_{\ell=1}^{\Lambda} \left[T_{\ell}^x T_{\ell+1}^x + T_{\ell}^y T_{\ell+1}^y + \Delta \left(T_{\ell}^z T_{\ell+1}^z - \frac{1}{4} \right) + H(-1)^{\ell} T_{\ell}^z \right], \quad (1)$$

where $\Delta > 1$ and the operators \mathbf{T}_{ℓ} satisfy the standard spin commutation relations; hence (1) may be thought of as the Hamiltonian of a ferromagnetic XXZ chain in a staggered magnetic field. A more physical interpretation is obtained by the canonical transformation $S_{\ell}^x = T_{\ell}^x$, $S_{\ell}^y = (-1)^{\ell} T_{\ell}^y$, $S_{\ell}^z = (-1)^{\ell} T_{\ell}^z$ which reduces (1) to a special limit of an antiferromagnetic XYZ Hamiltonian in a *uniform* field H . In view of the above dual interpretation we consider in parallel the two special operators

$$\tau = \sum_{\ell=1}^{\Lambda} T_{\ell}^z, \quad M = \sum_{\ell=1}^{\Lambda} (-1)^{\ell} T_{\ell}^z. \quad (2)$$

The operator τ is not endowed with a simple physical meaning but commutes with Hamiltonian (1) and thus provides a very useful classification of states. In contrast, the operator M does not commute with the Hamiltonian but represents the physical magnetization, a quantity of special interest in the following.

Although the main objective of this paper is to study the thermodynamic limit $\Lambda \rightarrow \infty$, some issues become clear by approaching that limit through a finite periodic chain with an even number of sites $\Lambda = 2N$. The eigenvalues of τ are then given by $\tau = 0, \pm 1, \dots, \pm N$ and split

the Hilbert space into $2N + 1$ sectors. The two extremal sectors $\tau = \pm N$ contain only one state each, which is an exact eigenstate of the Hamiltonian with energy $E = 0$ for any strength of the applied field H . In the original spin language these are the two completely polarized Néel states. To study their stability at finite H we also consider one-magnon excitations, with $\tau = -N + 1$ or $N - 1$, whose energy eigenvalues are the same for both sectors and are given explicitly by

$$E_k = \Delta \pm \sqrt{\cos^2(k/2) + H^2}, \quad G_{\pm} = \Delta \pm \sqrt{1 + H^2}, \quad (3)$$

where k is a sublattice crystal momentum. In Eq. (3) we also display the energies of the $k = 0$ modes, denoted by G_{\pm} , which will be referred to as the magnon gaps and are depicted in Fig. 1 as functions of the applied field.

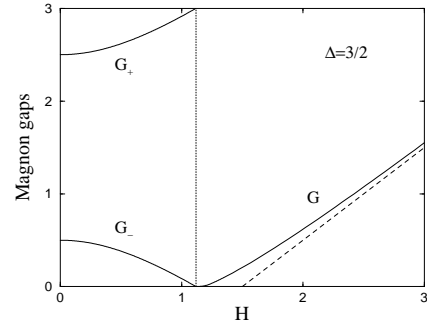


FIG. 1. Field dependence of the magnon gaps for the specific anisotropy $\Delta = 3/2$ for which the critical field is $H_b = 1.118$. The skew dashed line represents the Ising asymptote $H - \Delta$.

It is clear that the lowest gap closes ($G_- = 0$) at the critical field

$$H_b = \sqrt{\Delta^2 - 1} \quad (4)$$

beyond which the Néel states are no longer the lowest-energy states and the system undergoes a bulk spin-flop (BSF) transition.

The nature of this $T = 0$ phase transition is actually more interesting than indicated by the preceding argument. In fact, the lowest-energy states of *all* sectors become degenerate at the critical field, with energy $E = 0$, and the corresponding eigenstates can be constructed analytically.² For $H > H_b$ the $\tau = 0$ sector prevails in the sense that it contains the unique absolute ground state. Accordingly the first excited states are the lowest-energy states of the $\tau = \pm 1$ sectors and are degenerate. The corresponding magnon gap, denoted by G in Fig. 1, was computed via a Lanczos algorithm, on finite periodic chains with $\Lambda \leq 22$, complemented by straightforward Richardson extrapolation.³ The detailed numerical results indicate that the gap G might vanish through an essential singularity at H_b in the thermodynamic limit. Extrapolation becomes completely unnecessary for fields in the region $H \gtrsim \Delta$ where the gap G approaches the Ising asymptote $H - \Delta$. One would expect that the lowest gaps G_- and G dominate the low-temperature thermodynamics, in the respective field ranges, an issue that turned out to be more intricate than normally anticipated.

In order to prepare the discussion of thermodynamics it is also useful to calculate the magnetization M at $T = 0$. The magnetization vanishes for $H < H_b$ but exhibits a finite jump at the critical field which can be calculated analytically. For $H = H_b$ the expected value of M in the ground state $|\psi_\tau\rangle$ of each sector τ is

$$M_\tau = \frac{\langle \psi_\tau | M | \psi_\tau \rangle}{\langle \psi_\tau | \psi_\tau \rangle} = \sqrt{\Delta^2 - 1} \frac{N I_{N-1}}{I_N},$$

$$I_N = \frac{1}{\pi} \int_0^\pi \cos(\tau\theta) (\Delta + \cos\theta)^N d\theta, \quad (5)$$

which generalizes the $\tau = 0$ result quoted in Ref. 2. For any fixed τ a simple application of the Laplace method³ yields the asymptotic expansion

$$M_\tau = \left(N + \frac{1}{2}\right) \sqrt{\frac{\Delta - 1}{\Delta + 1}} + \frac{1 - 4\tau^2}{8N} \sqrt{\Delta^2 - 1} + O(1/N^2), \quad (6)$$

which can be used to extract the thermodynamic limit. Since the $\tau = 0$ sector contains the absolute ground state just above H_b , the magnetization jump at the critical field is given by

$$\mu_0 = \lim_{N \rightarrow \infty} \left(\frac{M_0}{2N} \right) = \frac{1}{2} \sqrt{\frac{\Delta - 1}{\Delta + 1}}. \quad (7)$$

A more subtle quantity is the $T = 0$ average magnetization at the critical point calculated from

$$\mu_b = \lim_{N \rightarrow \infty} \frac{1}{(2N)^2} \sum_{\tau=-N}^N M_\tau. \quad (8)$$

The asymptotic expansion (6) cannot be employed in Eq. (8) because the latter contains terms with values of τ that

are comparable to N . Nevertheless the explicit result (5) may be inserted in Eq. (8) to numerically estimate μ_b at large N .

For $H > H_b$ the $T = 0$ magnetization is not known analytically and we have again resorted to the Lanczos algorithm. At our maximum size $\Lambda = 22$ the Lanczos result for the magnetization jump at the critical field differs from the analytical prediction (7) by about 5%, a difference that is rectified by Richardson extrapolation to an accuracy about one part in a thousand. Hence we have applied the same extrapolation for $H > H_b$ and the result is depicted by a solid line in Fig. 2. Again, extrapolation becomes unnecessary for $H \gtrsim \Delta$.

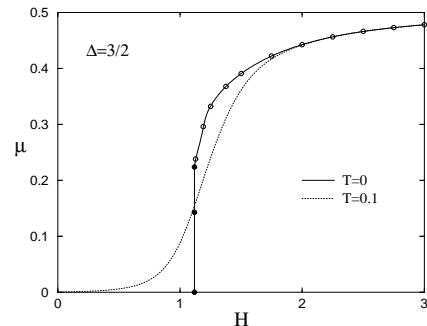


FIG. 2. Field dependence of the average magnetization per site $\mu = M/\Lambda$ for $T = 0$ (solid line) and $T = 0.1$ (dotted line). The solid circles represent the values of the $T = 0$ magnetization just below H_b ($\mu = 0$), right at H_b ($\mu_b = 0.143$), and just above H_b ($\mu_0 = 0.224$). The meaning of the open circles is discussed in the text.

We thus arrive at the main point of this paper, namely the calculation of thermodynamics via a TMRG algorithm⁴ which has already been applied to the study of quantum spin ladders⁵. One of the distinct features of the method is that it directly addresses the thermodynamic limit $\Lambda \rightarrow \infty$. We shall not present here numerical details but merely discuss some important results.

For instance, the temperature dependence of the magnetization is shown in Fig. 3 for a number of field values. The magnetization vanishes for all temperatures at vanishing field. For finite fields in the subcritical region, $H < H_b$, the magnetization again vanishes at $T = 0$, as expected, but develops a maximum at some finite temperature. Right at the critical field, $H = H_b$, the $T = 0$ limit of the calculated curve is consistent with the value $\mu_b = 0.143$ of Eq. (8), applied for $\Delta = 3/2$, whereas just above H_b the $T = 0$ limit is consistent with the value $\mu_0 = 0.224$ of Eq. (7). For supercritical fields, $H > H_b$, the low-temperature limiting values of μ extracted from Fig. 3 are depicted by open circles in Fig. 2 and are thus seen to be in excellent agreement with our independent Lanczos calculation of the magnetization at $T = 0$. Similarly the results extracted from Fig. 3 at the specific temperature $T = 0.1$ were used to calculate the field dependence of the magnetization at this temperature, a result that is shown by a dotted line in Fig. 2 and il-

illustrates the manner in which the $T = 0$ magnetization jump at the critical point is smoothed out at finite temperature.

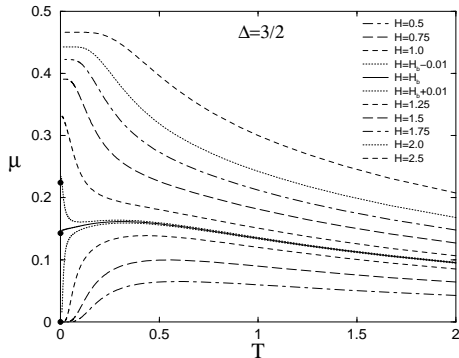


FIG. 3. Temperature dependence of the magnetization for various field values throughout the BSF transition. The solid circles on the μ axis correspond to the same values as those of Fig. 2.

We next turn our attention to the specific heat. In Fig. 4 we compare the TMRG result at vanishing field with a finite-size calculation for chains with $\Lambda = 10, 12$, and 14 for which a complete numerical diagonalization of the Hamiltonian is possible. This comparison is surprising in that the trend of the finite-size results does not seem to be consistent with the calculated thermodynamic limit. We have thus naturally questioned the validity of our TMRG calculation. However this special case was also considered in Fig. 4b of a paper by Klümper⁶ whose numerical method is again based on a transfer matrix but relies heavily on the complete integrability of model (1) at vanishing staggered field. Direct correspondence with the above author established that our result agrees with his throughout the temperature range considered.

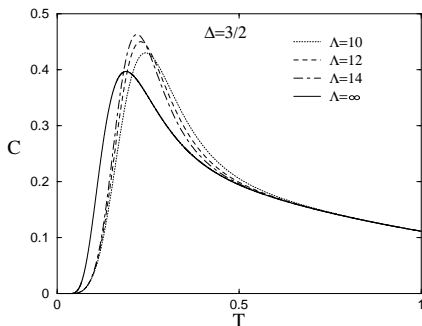


FIG. 4. Temperature dependence of the specific heat per site C at vanishing field ($H = 0$).

It should be added here that the TMRG method does not rely on complete integrability and is thus more flexible; e.g., it can be applied for the calculation of the thermodynamics at any finite staggered field for which model (1) is not known to be completely integrable.

The “anomalous scaling” observed in Fig. 4 for $H = 0$ persists for nonvanishing fields throughout the BSF tran-

sition but gradually disappears in the “no-scaling region” $H \gtrsim \Delta$ where the correct thermodynamic limit is practically reached by very short chains, as short as $\Lambda = 4$. In any case, the TMRG calculation of the temperature dependence of the specific heat is illustrated in Fig. 5 for various field values. The main feature of this figure is that the specific heat develops a double peak for fields in the vicinity of the critical point H_b . Furthermore the low-temperature behavior appears to be generally consistent with the field dependence of the magnon gaps shown in Fig. 1.

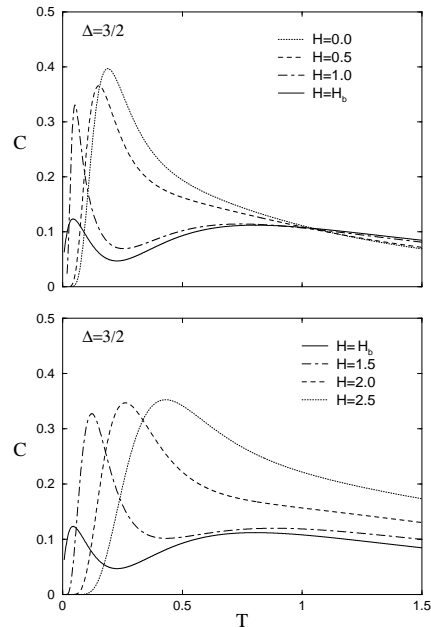


FIG. 5. Specific heat for various field values throughout the BSF transition.

One would expect that the low-temperature specific heat is correctly predicted by a dilute-magnon or spin-wave approximation, a long cherished assumption in condensed matter physics. To check this assumption we first consider the case of vanishing field for which our model is formally identical to the ferromagnetic XXZ chain extensively studied through the Bethe Ansatz^{6,7}. At sufficiently low temperature the spinwave approximation of the specific heat should read

$$C \approx \frac{G_-^2 \exp(-G_-/T)}{(2\pi T^3)^{1/2}}, \quad G_- = \Delta - 1, \quad (9)$$

where G_- is the lowest magnon gap at vanishing field. Equation (9) suggests considering the quantity $-T \ln(T^{3/2}C)$ which should interpolate linearly to the magnon gap G_- at $T = 0$. Yet a comparison of the spinwave prediction (9) with the TMRG calculation shown in the $\Delta = 3/2$ entry of Fig. 6 reveals a sharp disagreement even at the lowest temperature accessible by our method. On the other hand, one can show that the spinwave approximation agrees well with the finite-size results for $\Lambda = 10, 12, 14$ given in Fig. 4 restricted to the tempera-

ture range of Fig. 6. Clearly then the anomalous scaling noted earlier is intimately related to the apparent failure of the dilute-magnon approximation.

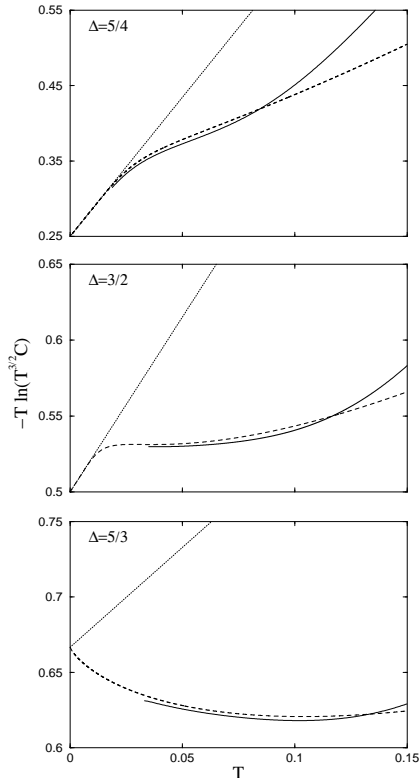


FIG. 6. Comparison of the calculated specific heat (solid line) at vanishing field ($H = 0$) with the spinwave approximation (9) (dotted line) and the Johnson-Bonner prediction (10) (dashed line).

In order to understand this situation we now invoke an asymptotic result obtained for the ferromagnetic XXZ chain by Johnson and Bonner⁷ who predict that the low-temperature specific heat is more appropriately described by

$$C \approx \frac{G_-^2 \exp(-G_-/T)}{(2\pi T^3)^{1/2}} + \frac{G_1^2 \exp(-G_1/T)}{T^2},$$

$$G_1 = \frac{1}{2} \sqrt{\Delta^2 - 1}, \quad (10)$$

where a new gap G_1 is potentially important. This gap originates in bound multimagnon or domain-wall states, including the notorious factor $1/2$ familiar from earlier discussions of the antiferromagnetic Ising and XXZ chains.⁸ The two terms in Eq. (10) may then be referred to as the magnon and Ising contributions, respectively. The two gaps G_- and G_1 become equal at the critical anisotropy $\Delta = 5/3$ and are ordered as $G_- < G_1$ or $G_- > G_1$ for $\Delta < 5/3$ or $\Delta > 5/3$.

Therefore, when $1 < \Delta < 5/3$, the magnon contribution in Eq. (10) dominates for sufficiently low temperature, practically in the region $T \ll G_1 - G_- \equiv \delta$. For $\Delta = 3/2$ one finds that $\delta = 0.06$ and hence the re-

gion $T \ll \delta$ is difficult to approach by the inherently finite-temperature TMRG algorithm. This explains the apparent failure of spinwave theory demonstrated in the $\Delta = 3/2$ entry of Fig. 6. However, when both terms of Eq. (10) are included, the agreement with our TMRG result is obviously very good. The picture becomes more transparent in the $\Delta = 5/4$ entry of Fig. 6 where the differential gap $\delta = 0.125$ is greater and thus the region $T \ll \delta$ becomes accessible to TMRG, albeit somewhat marginally. Also interesting is the result for the critical anisotropy $\Delta = 5/3$ shown in Fig. 6, where the failure of spinwave theory becomes complete, whereas our result continues to agree with the Johnson-Bonner prediction (10). Finally we have examined the case of a supercritical anisotropy, $\Delta = 2$, with a similar conclusion.

At finite (staggered) field our model is not equivalent to the ferromagnetic XXZ chain and thus the finite-field results of Ref. 7 are no longer applicable. We do not know at this point how to generalize Eq. (10) to account for a staggered field, especially because complete integrability seems to be lost. Numerical investigation of this issue suggests that spinwave anomalies persist in the subcritical region $H < H_b$ while normal spinwave behavior is restored for $H > H_b$. In the latter region the quantity $-T \ln(T^{3/2}C)$ interpolates linearly to the magnon gap G shown in Fig. 1.

To summarize, we have presented a reasonably complete theoretical description of the thermodynamics of the spin-flop transition for Hamiltonian (1). Our explicit results would be directly relevant for the analysis of actual experiments, provided that a quasi-one-dimensional magnetic system is found that is described by our model Hamiltonian at least approximately.⁹ Perhaps equally important is the overall conclusion that the TMRG method proves to be reliable even under stringent conditions.

We are grateful to A. Orendacova and M. Orendac for bringing Ref. 7 to our attention and for a related discussion. This work was completed during a visit of JK at IRRMA. XW and XZ acknowledge support by the Swiss National Foundation grant No. 20-49486.96, the Univ. of Fribourg and the Univ. of Neuchâtel. We would also like to thank A. Klümper for helpful correspondence.

¹ R.W. Wang, D.L. Mills, E.E. Fullerton, J.E. Mattson and S.D. Bader, Phys. Rev. Lett. **72**, 920 (1994).

² J. Karadamoglou and N. Papanicolaou, Phys. Rev. B **60**, 9477 (1999).

³ C.M. Bender and S.A. Orszag, *Advanced Mathematical Methods for Scientists and Engineers* (McGraw-Hill, New York, 1978).

⁴ X. Wang and T. Xiang, Phys. Rev. B **56**, 56 (1997).

⁵ X. Wang and L. Yu, cond-mat/9906399.

⁶ A. Klümper, Z. Phys. B **91**, 507 (1993).

⁷ J.D. Johnson and J.C. Bonner, Phys. Rev. B **22**, 251 (1980).

⁸ J.D. Johnson and B.M. McCoy, Phys. Rev. A **6**, 1613 (1972).

⁹ J. Kyriakidis and D. Loss, Phys. Rev. B **58**, 5568 (1998).